Yla-Herttuala et al. Journal of Cardiovascular Magnetic Resonance (2018) 20:34
https://doi.org/10.1186/s12968-018-0463-x

Journal of Cardiovascular Magnetic Resonance

RESEARCH Open Access

Quantification of myocardial infarct area based on T_{RAFFn} relaxation time maps - comparison with cardiovascular magnetic resonance late gadolinium enhancement, $T_{1\rho}$ and T_2 in vivo

Elias Yla-Herttuala[1], Svetlana Laidinen[1], Hanne Laakso[1,2] and Timo Liimatainen[3,4*]

Abstract

Background: Two days after myocardial infarction (MI), the infarct consists mostly on necrotic tissue, and the myocardium is transformed through granulation tissue to scar in two weeks after the onset of ischemia in mice. In the current work, we determined and optimized cardiovascular magnetic resonance (CMR) methods for the detection of MI size during the scar formation without contrast agents in mice.

Methods: We characterized MI and remote areas with rotating frame relaxation time mapping including relaxation along fictitious field in n^{th} rotating frame (RAFFn), $T_{1\rho}$ and T_2 relaxation time mappings at 1, 3, 7, and 21 days after MI. These results were compared to late gadolinium enhancement (LGE) and Sirius Red-stained histology sections, which were obtained at day 21 after MI.

Results: All relaxation time maps showed significant differences in relaxation time between the MI and remote area. Areas of increased signal intensities after gadolinium injection and areas with increased T_{RAFF2} relaxation time were highly correlated with the MI area determined from Sirius Red-stained histology sections (LGE: $R^2 = 0.92$, $P < 0.01$, T_{RAFF2}: $R^2 = 0.95$, $P < 0.001$). Infarct area determined based on $T_{1\rho}$ relaxation time correlated highly with Sirius Red histology sections ($R^2 = 0.97$, $P < 0.01$). The smallest overestimation of the LGE-defined MI area was obtained for T_{RAFF2} ($5.6 \pm 4.2\%$) while for $T_{1\rho}$ overestimation percentage was > 9% depending on $T_{1\rho}$ pulse power.

Conclusion: $T_{1\rho}$ and T_{RAFF2} relaxation time maps can be used to determine accurately MI area at various time points in the mouse heart. Determination of MI size based on T_{RAFF2} relaxation time maps could be performed without contrast agents, unlike LGE, and with lower specific absorption rate compared to on-resonance $T_{1\rho}$ relaxation time mapping.

Keywords: Cardiovascular magnetic resonance, Magnetic resonance imaging (MRI), Myocardial infarction (MI), Relaxation time, T_{RAFF2}, T_{RAFF4}, $T_{1\rho}$, T_2, LGE, Sirius red staining

* Correspondence: timo.liimatainen@oulu.fi
[3]Research Unit of Medical Imaging, Physics and Technology, University of Oulu, Oulu, Finland
[4]Department of Diagnostic Radiology, University Hospital of Oulu, P.O. Box 50, 90029 OYS Oulu, Finland
Full list of author information is available at the end of the article

Background

Cardiovascular diseases are the leading causes of death worldwide [1, 2]. Myocardial infarction (MI) is caused by a complete or partial blockage of the coronary artery, leading to inflammation, arrhythmia, and prolonged absence of perfusion [3–8]. The formation of fibrosis and collagen together with the loss of myocytes can lead to harmful remodeling of the myocardium and finally heart failure [3–7, 9]. Perfusion deficits cause cell death via necrosis and increases in extracellular space, which increases the tissue free water content and affects water-macromolecular interactions [10]. MI is a dynamic process since further loss of myocytes may occur, and collateral angiogenesis may decrease the infarct volume as a function of time [4, 6]. Scar tissue eventually replaces the damaged myocytes within 1–2 weeks after MI [4].

Several cardiovascular magnetic resonance (CMR) methods, for example T_2 and $T_{1\rho}$ relaxation time mappings and CMR spectroscopy, have been implemented to detect both acute and chronic MI [11–13]. Currently, the golden standard to detect chronic or irreversible injury using CMR is late gadolinium (Gd) enhancement (LGE). LGE creates a high contrast between normal myocardium and irreversible infarcted areas [11, 14, 15]. Contraindications for the use of Gd-based contrast agents are known Gd allergy and acute or chronic renal dysfunction [11, 16], which limit its clinical use.

Conventional transverse, or spin-spin, relaxation time, T_2, shows the difference between acute and chronic MI [15, 17]. Edema in the acute infarct phase increases free water content, significantly affecting heart function and T_2 relaxation time [12, 18]. Regions of acute MI can involve a mixture of tissue edema, hemorrhage, and inflammation, which leads to the underestimation of water movement in extracellular space and the overestimation of the infarct area in the T_2 relaxation time map [15, 19].

Rotating frame relaxation times are used to characterize the relaxation during radiofrequency (RF) pulses. This differs from conventional T_1 and T_2 relaxations where relaxation occurs during free precession. Longitudinal rotating frame relaxation time, $T_{1\rho}$, refers to relaxation along the RF field, which takes place typically during on-resonance RF irradiation. When RF irradiation is on-resonance and spins are locked along the RF field, the spins experience the RF field, instead of the main magnetic field. This leads to sensitivity of $T_{1\rho}$ to slow molecular motions with frequencies close to RF pulse frequency, which are typically in the range of 0.1 to 10 kHz in vivo. Comparatively, conventional T_1 is sensitive for Larmor frequency of the main magnetic field (B_0) which is typically in the range 10–500 MHz resembling high frequencies, i.e., fast molecular motions including the motion of free water. Increased $T_{1\rho}$ relaxation in MI has been associated with increased extracellular volume and alterations in proton exchange between water and macromolecules [11, 16]. Furthermore, $T_{1\rho}$ relaxation times are affected by macromolecule concentrations, viscosity, molecular weight and pH, since these factors change water mobility in tissue. Collectively, these factors affect molecular correlation times and therefore can explain $T_{1\rho}$ relaxation time increases in MI and other pathologies [16, 20]. Area with elevated $T_{1\rho}$ relaxation time show high correspondence with the MI area detected by LGE in mice [21] and in humans [11].

Specific absorption rate (SAR) often limits rotating frame relaxation measurements, especially in clinical settings, since high SAR may lead to tissue heating. One method to reduce SAR in rotating frame relaxation measurements is relaxation along a fictitious field (RAFF) in n^{th} rotating frame (RAFFn) [22–24]. RAFFn is produced by nested sine amplitude and cosine frequency modulated RF pulses operating in a sub-adiabatic regime and RF waveforms become more complicated when n increases [22, 23]. A fast, sub-adiabatic sweep of the effective RF field produces a fictitious field, which forms a part of the final effective RF field and magnetization precesses around this effective field [22]. When n increases in RAFFn, the tolerance for B_0 and radiofrequency field (B_1) inhomogeneities increases [23]. Due to lower flip angles with increasing n, the pulse bandwidth increases significantly [24]. Amplitude and frequency modulations, increase of bandwidth, decrease of flip angle together with remarkably lower (approximately 80%) SAR-values of RAFF4 and (approximately 30%) SAR-values of RAFF2 compared to continuous wave spin lock ($T_{1\rho}$) are clear advantages of RAFFn [22–24] and make RAFFn more suitable for clinical use than $T_{1\rho}$.

In the current study, we have optimized infarct sizing using T_{RAFF2} and T_{RAFF4} relaxation time mappings. The results were compared with $T_{1\rho}$ and T_2 relaxation time mappings, LGE and histology staining with Sirius Red.

Methods

Animal model

The left anterior descending artery (LAD) was ligated permanently in 10 female C57BL mice (20-24 g) as previously described [25]. Mice were anesthetized by 4% of isoflurane (Piramal Healthcare, Northumberland, UK), and anesthesia was maintained with 2.0% during the operation. The left side of mouse chest from sternum to Linea axillaris posterior was shaved and disinfected with 75% ethanol. An approximately 1.5 cm long transversal incision was made at the level of the fourth rib to left intercostal space. Through the incision and with help of a self-retaining retractor, the heart was exposed. The LAD was ligated with a 6.0 silk suture approximately at midway between its origin and the apex of the heart.

After the LAD ligation, the heart was placed back to its original location. The skin were sutured in layers with 5.0 nylon suture. After the surgery, 0.05–0.1 mg/kg buprenorphine (0.3 mg/ml Temgesic, RB Pharmaceuticals, Slough, UK) and 5 mg/kg carprofen (50 mg/ml, Rimadyl, Pfizer Oy Animal Health, Helsinki, Finland) for analgesia were injected subcutaneously and repeated at days 1 and 2 after the surgery. All surgical procedures were performed according to protocols approved by the Finnish Committee for the use and care of laboratory animals.

CMR

Mice underwent CMR at 1 ($n = 10$), 3 ($n = 9$), 7 ($n = 5$) and 21 ($n = 5$) days after LAD occlusion. All experiments were performed using a horizontal 9.4 T magnet (Varian Inc. Palo Alto, California, USA) with a gradient set with maximum gradient strength of 600 mT/m and controlled by a Bruker console (Bruker GmbH, Ettlingen, Germany). Quadrature volume transceiver with a coil diameter of 35 mm (Rapid Biomed GmbH, Ettlingen, Germany) was used for all CMR experiments. Mice were anesthetized for CMR with 4% isoflurane mixed in oxygen and nitrogen with ratio of 1:3. The level of isoflurane was decreased to 1% for the imaging. Mouse body temperature was kept close to 37 °C by circulating warm water tubes placed under the mouse. Electrocardiography (ECG) was measured from fore paws using needle electrodes and a pneumatic pillow placed under the mouse monitored respiration. Both signals were registered using Model 1025 monitoring and gating system (Small Animal Instruments Inc., Stony Brook, New York, USA) during the experiments. Both ECG and respiration signals were used to gate CMR experiments.

Multi-slice cine images covering the whole heart were taken using fast imaging with balanced steady state precession (FISP) readout sequence. The imaging parameters for cine images were FOV = 4 × 4 cm^2, slice thickness = 1 mm, matrix size = 192 × 192, TE = 1.9 ms, TR = 8.0 ms, scan TR = 99.0 ms, flip angle = 10° and number of frames 10–11 depending on mouse heart rate. Depending on the size of the heart, 8–10 slices were imaged.

The rotating frame preparation modules used to measure T_{RAFFn} consisted of RAFF2 or RAFF4 pulses (pulses RF power ($\gamma B_1/(2\pi)$) 1250 Hz and 648 Hz, respectively, duration 2.26 ms) which were applied in pulse trains of lengths 0, 9.1, 18.1 and 36.2 ms. Before the RAFFn pulse train, a delay with durations of 36.2, 27.15, 18.1 and 0 ms, respectively, was added to adjust imaging to occur at the same cardiac phase for weightings with different durations. An illustration of a rotating frame preparation module and readout sequence is shown in Fig. 1.

$T_{1\rho}$ preparation was performed using a rotating frame preparation module (Fig. 1) which contained adiabatic half passage (AHP) pulse (power 1250 Hz, duration 2.0 ms), continuous wave spin-lock-pulse with time-to-spin-lock (TSL) = 0.4, 9.4, 27.4 and 45.4 ms and AHP-back pulse (power 1250 Hz, duration 2.0 ms) [21]. Before $T_{1\rho}$ preparation a delay (45.4, 27.4, 9.4 and 0 ms, respectively to TSL) was added. $T_{1\rho}$ dispersion was measured by altering the spin lock power ($\gamma B_1/(2\pi)$) in a range of (400, 625 and 1250 Hz) and keeping AHP and AHP-back pulses the same.

T_2 measurements were conducted using Hahn double echo preparation containing an AHP excitation-pulse (power 1250 Hz, duration 3.0 ms), two Hyperbolic Secant (HS1)-pulses (power 1250 Hz, duration 4.5 ms) and a reversed AHP-pulse (power 1250 Hz, duration 3.0 ms) (Fig. 1). Between the pulses symmetric delays were used resulting in total TEs of 0.05, 2.3, 4.5, and 14.0 ms. Delays in front of T_2 preparation were 14.0, 4.5, 2.3 and 0.05 ms, respectively.

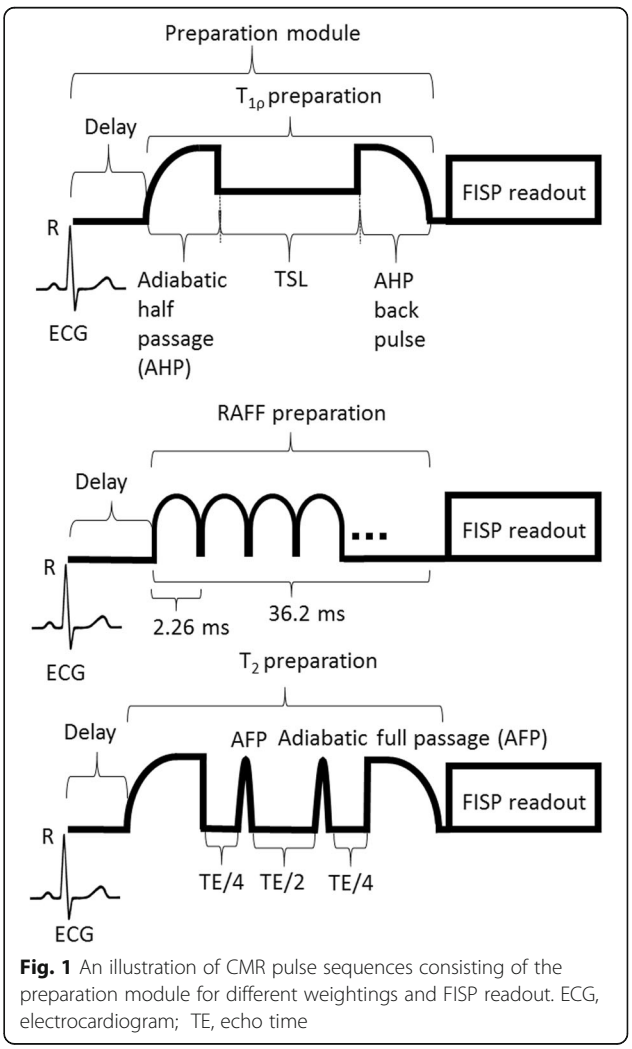

Fig. 1 An illustration of CMR pulse sequences consisting of the preparation module for different weightings and FISP readout. ECG, electrocardiogram; TE, echo time

B_1 was measured by applying a block pulse with power of 625 Hz. The B_1 block pulse was applied with pulse durations 0, 0.25, 0.5, 0.75, 1.0, 1.25, 1.5 and 1.75 ms [26].

All relaxation time maps and B_1 measurements were acquired using a FISP-readout sequence in a single short-axis slice at the mid-ventricular level. The following parameters: FOV = 4 × 4 cm^2, slice thickness = 1 mm, matrix size = 256 × 256 (for B_1 measurements, the matrix size was 128 × 128), TE = 1.9 ms, TR = 14.9 ms, and flip angle = 90° were used for the FISP-readout. A delay between weighting pulses depended on respiratory rate being at least 1460 ms.

At the last time point before sacrificing the mice, LGE images were acquired in the same slice as all other measurements using an inversion prepared pulse sequence with an inversion time of 300 ms, FISP-readout, FOV = 4 × 4 cm^2, slice thickness = 1 mm, matrix size = 256 × 192, TE = 2.0 ms, TR = 5.6 ms, scan TR = 3000.0 ms and flip angle = 90° [27]. The gadobutrol (Gadovist, Bayern Oy, Turku, Finland) intravenous injection volume was 5 ml/kg per mouse.

Only five mice survived to 21 days and were sacrificed for histology after imaging. For histology, the hearts were perfused through the left ventricle with phosphate buffered saline and then immersion fixed with 4% paraformaldehyde with sucrose in phosphate buffered solution for 4 h. After 4 h, the hearts were placed into 15% sucrose. Paraffin-embedded, 4 μm thick, cross-sections of the heart were stained with Sirius Red to determine the fibrotic areas of the infarcted myocardium. Histological sections were analyzed and photographed with microscopy (Nikon Eclipse, Ni-E, Tokyo, Japan).

Data analysis

All relaxation time maps were reconstructed from signal intensities with pixel-by-pixel analysis using Aedes software package (http://aedes.uef.fi/) in Matlab platform (Mathworks Inc. Natick, Massachusetts, USA). $T_{1\rho}$ and T_2 relaxation time maps were fitted using linear function for linearized data. T_{RAFF2} and T_{RAFF4} were fitted by using single mono-exponential decay function without taking into account the steady state formation. Regions of interest (ROIs) were manually traced with visual delineations of MI and remote areas based on relaxation time maps, cine images and images of Sirius Red-stained sections. End systolic volume (ESV), end diastolic volume (EDV), ejection fraction (EF), and cardiac output (CO) were defined based on endocardial border in cine images.

Infarct percentage analysis was done with midline length-based method with a function of $(L_{(infarct)}/ L_{(circumference)})$•100%, where L denotes measured length from either T_{RAFF2}, T_{RAFF4}, $T_{1\rho}$, T_2, LGE or Sirius Red-stained section [28]. Relative relaxation time difference (RRTD) values were calculated with function of $(T_{(infarct)} - T_{(remote)})/ T_{(remote)}$, where T denotes either T_{RAFF2}, T_{RAFF4}, $T_{1\rho}$ or T_2 relaxation time.

Amount of overestimation (AOE) of infarct area relative to the LGE-defined MI area, as the gold standard, was calculated based on midline length-based method with a function of $((L_{(infarct)} - LGE_{(infarct)})/ L_{(infarct)})$ •100%, where L denotes either T_{RAFF2}, T_{RAFF4}, $T_{1\rho}$ or T_2 relaxation time [29].

Statistics: All numerical values are given as mean ± standard deviation (SD). Two-way ANOVA with Bonferroni post hoc testing was applied to compare the spatial and temporal changes between the infarct and remote areas of myocardium, and the analyses were performed using GraphPad Prism software (GraphPad Software, La Jolla, California, USA). Two-way ANOVA with Bonferroni post hoc testing was performed to compare changes between RRTD values of different relaxation times. One-way ANOVA with Bonferroni post hoc testing for multiple comparisons were applied to compare time point differences between relaxation times and also the differences between time points of cardiac functions.

Results

Increased relaxation time constants were found in the MI areas after LAD ligation. Infarct areas obtained with relaxation time mappings were compared with infarct areas derived based on LGE-images, cine-images and Sirius Red-stained histological sections (Fig. 2).

T_{RAFF2} relaxation times were significantly higher in the infarct areas compared to remote areas ($P < 0.001$) (Fig. 3a). T_{RAFF2} relaxation times in infarct area increased significantly up to 7 days and remained elevated until day 21 after the LAD ligation ($P < 0.05$, $P < 0.05$, respectively) (Fig. 3a). T_{RAFF4} relaxation time in the infarct area was significantly elevated at all time points compared to the remote area ($P < 0.001$, Fig. 3b). The remaining relaxation times ($T_{1\rho1250}$, $T_{1\rho625}$, $T_{1\rho400}$ and T_2) were significantly elevated in the infarct area compared to remote areas ($P < 0.001$, respectively), and there were significant differences, except in $T_{1\rho1250}$, between time points ($P < 0.05$, respectively, Fig. 3c-f). Specifically, $T_{1\rho625}$ relaxation times increased significantly in the infarct area at 7 days after the LAD ligation ($P < 0.01$) and remained elevated until day 21 ($P < 0.001$, Fig. 3e). There was a significant increase in $T_{1\rho625}$ relaxation times in infarct area at days 7 and 21 compared to day 1 after the LAD occlusion ($P < 0.05$, $P < 0.05$ respectively), and it also increased significantly from day 3 to day 21 ($P < 0.05$, Fig. 3e). Additionally, the trend between infarct and remote areas in $T_{1\rho625}$, $T_{1\rho400}$ and T_2 relaxation times differed significantly ($P < 0.05$, respectively) from each other (Fig. 3c, e, f). A decrease in T_2 relaxation time was detected from day 3 to day 21 after the LAD ligation ($P < 0.05$, Fig. 3c).

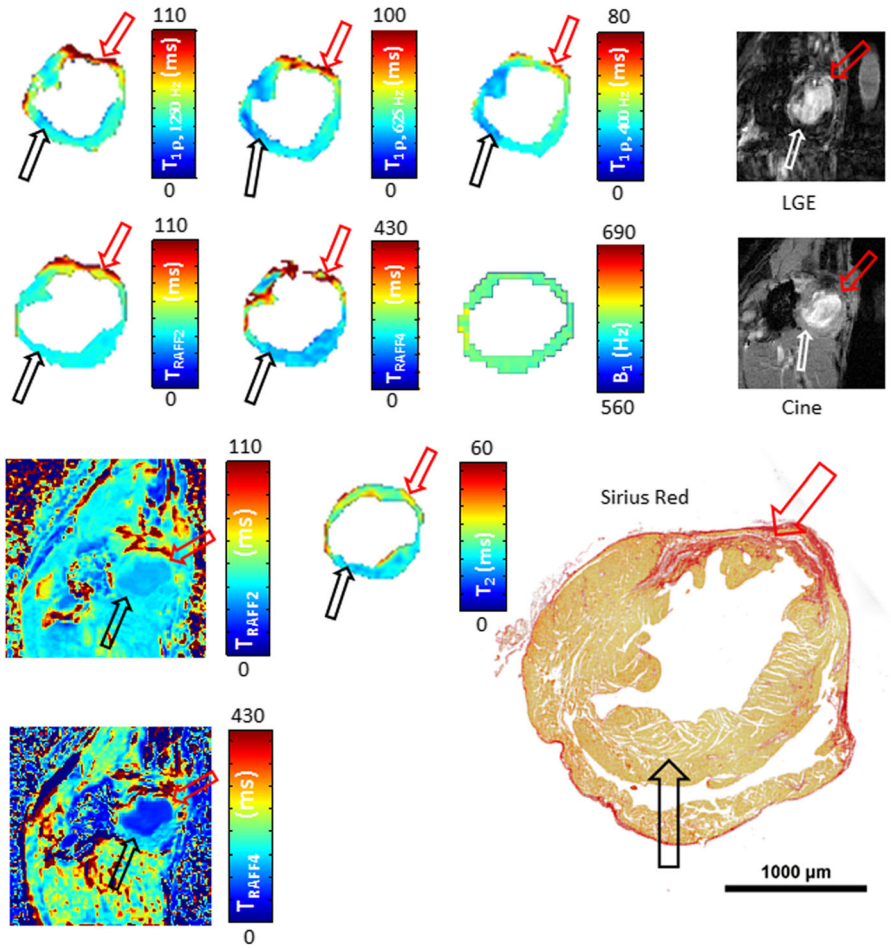

Fig. 2 Relaxation time maps, late gadolinium enhancement (LGE), cine and a corresponding histology image with Sirius Red-stained section from infarcted mouse heart at the last (21 day) time point after left anterior descending (LAD) myocardial infarction (MI). Red arrows indicate the infarct area and black/white arrows show the remote control area. B_1 homogeneity was verified to be nominal ±10% Hz in the area of the whole myocardium

There were no significant changes in the relaxation times in the remote areas between the imaging time points ($P > 0.05$, Fig. 3).

RRTD provided a measure of differences in relaxation time values between infarct and remote areas for the relaxation measurements (Table 1). RRTD values of T_{RAFF4} differed significantly from other relaxation time methods at several different time points (Table 1). There were significant differences in RRTD values of some of the $T_{1\rho}$ relaxation times when comparing RRTD values at day 1 (Table 1).

AOE values were determined for all relaxation times (Fig. 4a). AOE was lowest for T_{RAFF2} indicating that area of increased T_{RAFF2} is most similar to LGE-measured infarct area (Fig. 4a).

Infarct sizes were calculated also as a ratio between the arc of infarct and the circumference of the whole myocardium from relaxation time maps and LGE-images (Figs. 4b and 5). These infarct sizes were correlated with the ones measured based on Sirius Red-stained histology-images (Fig. 5). The highest Spearman correlations were obtained with $T_{1\rho}$ ($R^2 = 0.97$, $P < 0.01$). Infarct sizes from T_{RAFF2} ($R^2 = 0.93$, $P < 0.001$) and T_{RAFF4} ($R^2 = 0.94$, $P < 0.001$) showed a high correlation as well as LGE ($R^2 = 0.92$, $P < 0.01$) with infarct size from Sirius Red-stained sections (Fig. 5). The infarct fraction given as a percentage at early time points obtained from T_2 relaxation time map was largest but decreased to similar percentages as obtained from the other relaxation time maps at day 21 (Fig. 4b).

Dispersion of $T_{1\rho}$ relaxation times ($\Delta T_{1\rho}$) was calculated by subtracting $T_{1\rho}$ relaxation times measured with different spin lock powers (Fig. 6). Significant differences between different $T_{1\rho}$ relaxation times in infarct and remote areas were not found, and the difference in both areas remained almost constant between the time points (Fig. 6).

Parameters of cardiac function indicate that MI has developed as a function of time (Table 2). Specifically EF decreased as a function of time and, three weeks after

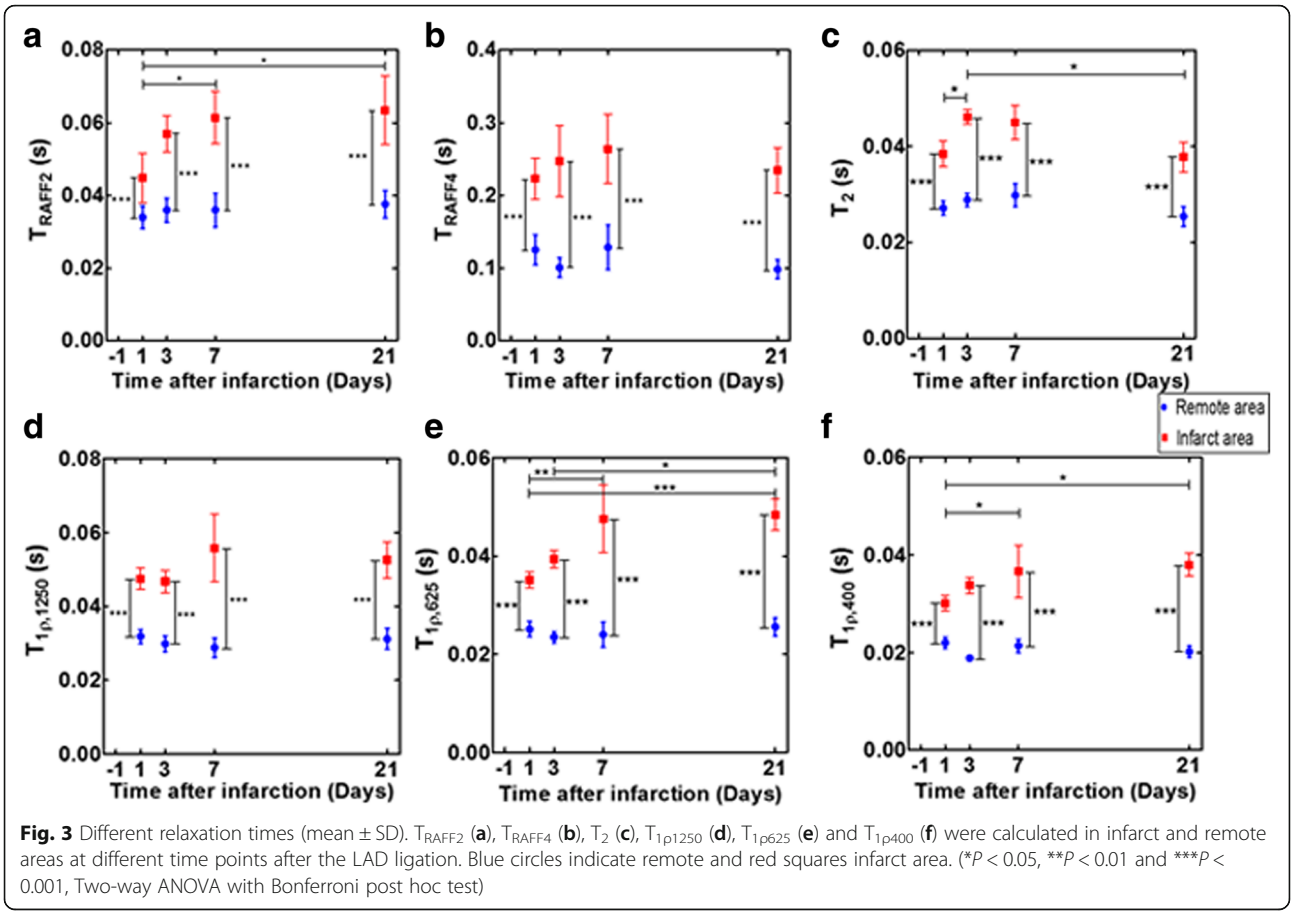

Fig. 3 Different relaxation times (mean ± SD). T_{RAFF2} (**a**), T_{RAFF4} (**b**), T_2 (**c**), $T_{1\rho1250}$ (**d**), $T_{1\rho625}$ (**e**) and $T_{1\rho400}$ (**f**) were calculated in infarct and remote areas at different time points after the LAD ligation. Blue circles indicate remote and red squares infarct area. (*$P < 0.05$, **$P < 0.01$ and ***$P < 0.001$, Two-way ANOVA with Bonferroni post hoc test)

MI, EF had decreased to 0.35 (Table 2). Increased cardiac output between days 1 and 7 was found, although it was assumed to decrease (Table 2).

Discussion

In this murine study, relaxation times were measured in infarct and remote areas at several time points after MI. Infarct size was measured based on different relaxation times, the results were compared to infarct sizes derived from CMR LGE-image and Sirius Red-stained histology sections. MI size from $T_{1\rho}$, T_{RAFF2} and T_{RAFF4} relaxation time maps showed a high correlation with MI size determined based on Sirius Red-stained histology sections.

T_{RAFF2} relaxation times in infarct areas increased significantly from day 1 to day 21 after the LAD ligation and the RRTD values increased as a function of time. Differences between infarct and remote areas in T_{RAFF2} relaxation times were statistically significant. Low AOE-value obtained with T_{RAFF2} relaxation time demonstrate that elevated T_{RAFF2} denotes permanently damaged area. These findings together with a high

Table 1 Relative relaxation time difference (RRTD) values formed by infarct and remote area relaxation times presented as mean ± SD

Relaxation time constant	Day 1	Day 3	Day 7	Day 21
$T_{1\rho1250}$	0.49 ± 0.11$^{\square}$	0.60 ± 0.29$^{\square\square\square}$	0.91 ± 0.42*	0.69 ± 0.16$^{\square\square}$
$T_{1\rho625}$	0.41 ± 0.09$^{\square\square}$	0.70 ± 0.27$^{\square\square\square}$	0.99 ± 0.44**	0.90 ± 0.24*
$T_{1\rho400}$	0.37 ± 0.09$^{\square\square}$	0.79 ± 0.21**,$^{\square\square}$	0.69 ± 0.33$^{\square}$	0.90 ± 0.27**
T_2	0.41 ± 0.11$^{\square\square}$	0.61 ± 0.19$^{\square\square\square}$	0.51 ± 0.11$^{\square\square}$	0.50 ± 0.19$^{\square\square\square}$
T_{RAFF2}	0.41 ± 0.12$^{\square\square}$	0.62 ± 0.43$^{\square\square\square}$	0.73 ± 0.22	0.66 ± 0.21$^{\square\square}$
T_{RAFF4}	0.90 ± 0.45	1.36 ± 0.62	1.22 ± 0.59	1.39 ± 0.37

Significance of differences in RRTD values were calculated by Two-way ANOVA with Bonferroni post hoc test ($^{\square}$=P<0.05, $^{\square\square}$=P<0.01, $^{\square\square\square}$=P<0.001 for difference to T_{RAFF4} at that specific time point) and One-way ANOVA with Bonferroni post hoc test (*=P<0.05, **=P<0.01 for difference to day 1)

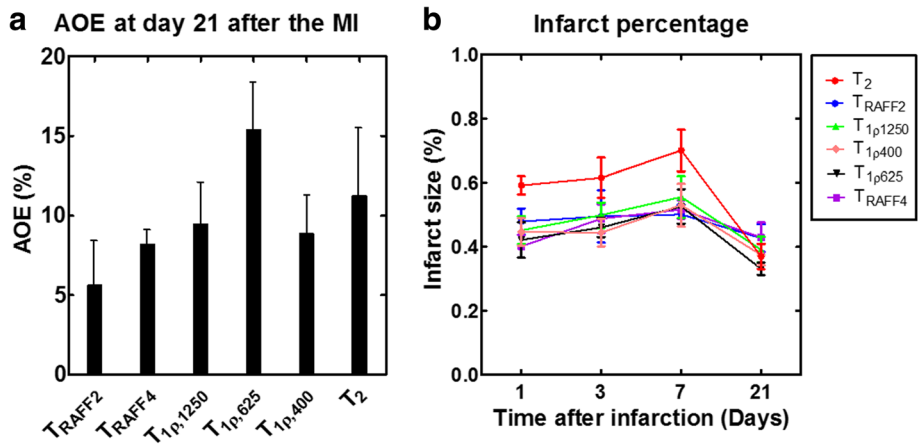

Fig. 4 Amount of overestimation (AOE) with regard to the LGE-defined MI area based on the relaxation time maps at 21 days after infarct (**a**) and infarct percentages at every time point based on the relaxation time maps (**b**)

correlation between T_{RAFF2} and histology derived infarct size, demonstrate that T_{RAFF2} relaxation time detects MI area with high accuracy. Previously, T_{RAFF2} relaxation time has been measured in a rat malignant glioma model where T_{RAFF2} showed a high correlation with decreased cell density in tumors [30]. Furthermore, cell density decreases in the infarct area as the tissue is replaced by fibrotic tissue, which leads to an increase of extracellular space [10]. Most likely, increase of T_{RAFF2} in both of these cases is caused by increases in extracellular space and, therefore, an increase in free water content. This suggest that fibrotic tissue can be differentiated healthy tissue using the T_{RAFF2} map. This is important since fibrosis detection also plays a central role in MI detection. Our results demonstrate the potential of T_{RAFF2} mapping to determine and accurately assess the MI area in both acute and chronic phase of the disease. Another explanation for elevated T_{RAFF2} is altered ^{1}H chemical exchange between water and macromolecules due to changes induced by infarct in exchange of populations,

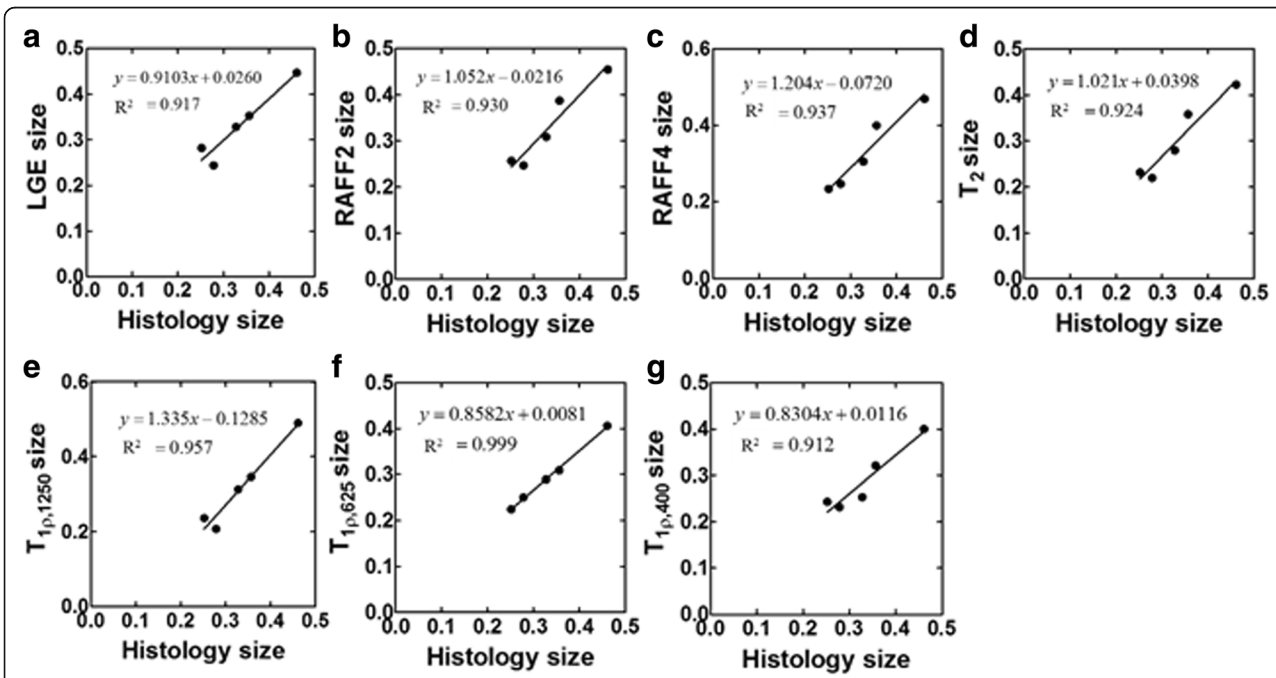

Fig. 5 Linear correlation from the ratios between the arc of infarct and the circumferences of the whole myocardium determined from LGE-image (**a**), T_{RAFF2} (**b**), T_{RAFF4} (**c**), T_2 (**d**), $T_{1\rho1250}$ (**e**), $T_{1\rho625}$ (**f**), $T_{1\rho400}$ (**g**) and Sirius Red-stained histology sections. Formulas of linear relationships are shown next to correlation line

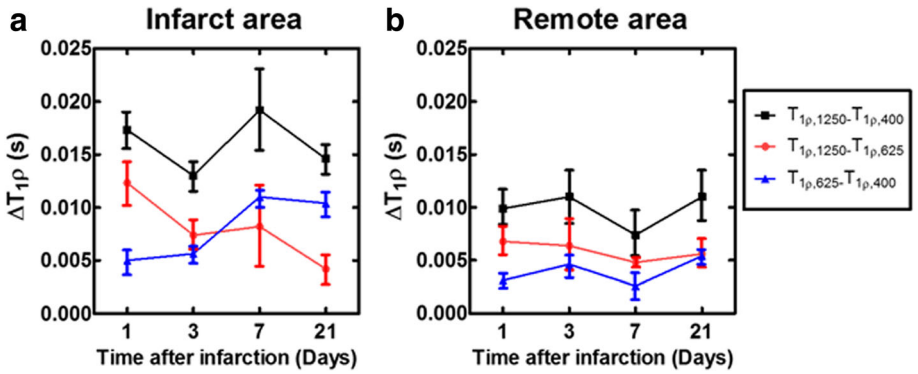

Fig. 6 Dispersion of $T_{1\rho}$ relaxation time in infarct area (**a**) and in remote area (**b**). Red color shows subtraction between $T_{1\rho1250}$ - $T_{1\rho625}$, black color shows subtraction between $T_{1\rho1250}$ - $T_{1\rho400}$ and blue color shows subtraction between $T_{1\rho625}$ - $T_{1\rho400}$

exchange rates, or chemical shifts between exchanging sites [30]. The extracellular pH may also change in MI, which may induce alterations to exchange rates [30].

Our results showed that T_{RAFF4} relaxation times were elevated at all time points in the MI area and the difference between infarct and remote areas in T_{RAFF4} was significant. Our findings suggest that T_{RAFF4} relaxation time mapping can be applied to detect chronic MI since infarct size derived from T_{RAFF4} map correlated highly ($R^2 = 0.94$, $P < 0.001$) with histology derived infarct area together with small AOE-value.

$T_{1\rho1250}$ relaxation time determined at infarct area was significantly higher when compared to remote areas of the myocardium. In addition, infarct size derived from $T_{1\rho1250}$ map correlated with infarct size from Sirius Red sections ($R^2 = 0.96$, $P < 0.01$) and its AOE-value was close to zero. The largest RRTD between infarct and remote area was found with $T_{1\rho625}$. Infarct size based on $T_{1\rho625}$ and $T_{1\rho400}$ relaxation time maps showed high correlations ($R^2 = 0.99$, $P < 0.001$, $R^2 = 0.96$, $P < 0.05$, respectively) with Sirius Red staining but $T_{1\rho625}$ showed the largest AOE-value (15.4 ± 6.1%). $T_{1\rho}$ relaxation times have previously been known to be two times longer in scar tissue than in normal myocardium in porcine heart [16]. However, the origin of $T_{1\rho}$ increase at MI is still unclear. Most likely it is due to increased fibrosis content, cellularity, or ^{1}H chemical exchange [11, 31]. In addition, there is a suggestion that leaking protein material from sarcolemma into extracellular space minimizes effects of proteins on water molecules or macromolecules in acute MI in patients and swine [10, 17]. Selective sensitivity to correlation times near to $1/(\gamma B_1)$ is an advantage of $T_{1\rho}$ relaxation time [21].

In a previous study, the $T_{1\rho}$ relaxation time with different spin-lock powers increased significantly 7 days after MI compared to the remote area [21] and $T_{1\rho}$ relaxation times elevated almost monotonically during 2 weeks after MI [21]. These findings were explained by granulation and scar tissue formation [11, 21]. Similar increase was detected in this study with $T_{1\rho}$s, T_{RAFF2}, and T_{RAFF4}.

T_2 relaxation times increased significantly from day 1 to day 3 in infarct area and T_2 relaxation times in infarct area were significantly higher than T_2 relaxation times in remote area. These results are in line with previous findings showing that damaged area in myocardium is reversible in acute phase of MI [12, 18, 32]. It has previously been shown that T_2 relaxation time overestimates the size of acute MI compared to chronic MI, since the inflammation and edema have resolved from the chronic MI [18]. Similar findings were observed in this study since infarct percentages based on T_2 maps were higher as compared to percentages based on the other relaxation times at early time points. Therefore, increased T_2 relaxation time shows the area of edema rather than the

Table 2 Values of cardiac function parameters which are presented as mean ± SD

Cardiac function parameters	Day 1	Day 3	Day 7	Day 21
End diastolic volume (mm^3)	48.4 ± 20.7	47.1 ± 24.6	72.9 ± 26.7	90.3 ± 30.2*,□
End systolic volume (mm^3)	22.7 ± 13.0	21.9 ± 13.8	39.9 ± 17.6	58.0 ± 18.5**,□□
Ejection Fraction (%)	0.55 ± 0.12	0.56 ± 0.09	0.46 ± 0.09	0.35 ± 0.04**,□□
Cardiac output (mm^3)	14,570 ± 3680	15,140 ± 5770	20,280 ± 8130*	19,800 ± 8680
Heart rate (bpm)	580.2 ± 82.5	599.0 ± 64.9	615.5 ± 48.0	632.0 ± 52.3

Differences between time points of different cardiac measures were analyzed by One-way ANOVA with Bonferroni post hoc test (*=P<0.05 for difference to day 1) (□=P<0.05, □□=P<0.01 for difference to day 3)

actual size of MI [18]. T_2 relaxation times did not differ between day 1 and day 21, which suggests that part of the damage in myocardium was reversible without the scar formation. In a previous study, T_2 relaxation times were significantly higher in acute MI area compared to chronic MI area [12].

The MI areas defined based on CMR images were in good agreement with the areas determined with Sirius Red-stained histology. To our knowledge, elevated relaxation times, at least $T_{1\rho}$ relaxation times, at 21 days after MI are due to fibrosis and scar tissue formation. The locations of fibrotic areas in Sirius Red-stained sections and the elevated relaxation times on relaxation time maps agreed well. Notable, our results are based on quantitative relaxation times instead of weighted images. These results also suggest that especially T_{RAFF2}, T_{RAFF4} and $T_{1\rho}$ relaxation time mappings may be useful for broad range of clinical applications where myocardial tissue characterization is needed, for example in myocarditis, various size and locations of scars, sarcoidosis and hypertrophy. Operating at lower main magnetic field strengths will have some impact on rotating frame relaxation times; however, the main influence is the strength of the spin-lock power [33]. Water molecules with correlation times close to $1/(\gamma B_1)$ contribute to rotating frame contrasts [33]. Adaption of rotating frame measurements to MI characterization at clinics needs further study since we demonstrated advantages of relaxation times only in MI mouse model where one artery (LAD) was occluded.

MI area was detectable in all relaxation time maps and it was the most visible at day 21. At the first time points, the MI area was larger than at the later time points most likely due to inflammation surrounding the infarction area. In a mouse model, MI area consists of over 90% of necrotic tissue only two days after LAD ligation and the necrotic tissue is transformed into granulation tissue one week after MI and into scar two weeks after the LAD ligation [5].

The LAD ligations were successfully performed since our results show a clear visibility of infarct in Sirius Red-stained sections and decreased EF values as a function of time. Additionally, EDV and ESV tend to increase post MI due to changes in physiology of the myocardium. Changes in physiology with decreased perfusion inside the myocardium lead also to a decrease of EF as a function of time. Our EF values agreed with EF values reported in the literature [34, 35]. Increased EDV and ESV at day 21 compared to day 1 after MI resulted in an increased stroke volume (23%) which together with increased heart rate (8%) lead to increased cardiac output. The ventricular dilation after MI is typical [34, 35] and was also observed in our cine images. However, increased stroke volume after MI is rare [34, 35]. Differences in anesthesia level or mice increased tolerance to anesthetic during subsequent CMR exams might be the reasons for the increased heart rates.

Conclusions

All relaxation time maps showed high contrast between infarct and remote areas. $T_{1\rho}$, T_{RAFF2} and T_{RAFF4} relaxation time maps correlated significantly with the infarct size determined by histology. As a conclusion, T_{RAFF2} and T_{RAFF4} relaxation time maps can be used to accurately determine infarct size in mouse myocardial infarct without the use of contrast agent with clinically tolerable specific absorption rates.

Abbreviations

AHP: Adiabatic half passage; AOE: Amount of overestimation; CMR: Cardiovascular magnetic resonance; CO: Cardiac output; ECG: Electrocardiogram; EDV: End-diastolic volume; EF: Ejection fraction; ESV: End-systolic volume; Gd: Gadolinium; LAD: Left anterior descending coronary artery; LGE: Late gadolinium enhancement; MI: Myocardial infarction; RAFF: Relaxation along a fictitious field; RF: Radiofrequency; ROI: Region of interest; RRTD: Relative relaxation time difference; SAR: Specific absorption rate; TSL: Time to spin lock

Acknowledgements

The authors thank Maarit Pulkkinen for technical assistance. The authors thank Nicholas Downes for checking the language of the manuscript.

Funding

Sigrid Juselius foundation and University of Eastern Finland Doctoral Programme of Molecular Medicine.

Availability of data and materials

The datasets used and/or analyzed during the current study are available from the corresponding author on reasonable request.

Authors' contributions

Each author contributed significantly to the submitted work: EYH was involved in the design of the study, performed CMR measurements, performed data analysis, interpreted the data and drafted the manuscript. SL did LAD surgeries, histology and revised the manuscript. HL helped to design CMR measurements, helped in CMR measurements and revised the manuscript. TL designed the study and revised the manuscript. All authors read and approved the final manuscript.

Ethics approval and consent to participate

All surgical procedures were performed according to protocols approved by the Finnish Committee for the use and care of laboratory animals.

Competing interests

The authors declare that they have no competing interests.

Publisher's Note

Author details

[1]A.I. Virtanen Institute for Molecular Sciences, University of Eastern Finland, Kuopio, Finland. [2]Center for Magnetic Resonance Research, Minneapolis, MN, USA. [3]Research Unit of Medical Imaging, Physics and Technology, University of Oulu, Oulu, Finland. [4]Department of Diagnostic Radiology, University Hospital of Oulu, P.O. Box 50, 90029 OYS Oulu, Finland.

Received: 12 September 2017 Accepted: 24 May 2018
Published online: 07 June 2018

References

1. Ylä-Herttuala S, Bridges C, Katz MG, Korpisalo P. Angiogennic gene therapy in cardiovascular diseases: dream or vision? Eur Heart J. 2017;38:1365–71.
2. Ylä-Herttuala S, Baker AH. Cardiovascular gene therapy: past, present, and future. Mol Ther. 2017;25:1095–106.
3. Blankesteijn WM, Creemers E, Lutgens E, Cleutjens JP, Daemen MJ, Smits JF. Dynamics of cardiac wound healing following myocardial infarction: observations in genetically altered mice. Acta Physiol Scand. 2001;173:75–82.
4. Ertl G, Frantz S. Healing after myocardial infarction. Cardiovasc Res. 2005;66:22–32.
5. Virag JI, Murry CE. Myofibroblast and endothelial cell proliferation during murine myocardial infarct repair. Am J Pathol. 2003;163:2433–40.
6. Holmes JW, Yamashita H, Waldman LK, Covell JW. Scar remodeling and transmural deformation after infarction in the pig. Circulation. 1994;90:411–20.
7. McKay RG, Pfeffer MA, Pasternak RC, Markis JE, Come PC, Nakao S, Alderman JD, Ferguson JJ, Safian RD, Grossman W. Left ventricular remodeling after myocardial infarction: a corollary to infarct expansion. Circulation. 1986;74:693–702.
8. Frangogiannis NG, Smith CW, Entman ML. The inflammatory response in myocardial infarction. Cardiovasc Res. 2002;53:31–47.
9. Gaudron P, Kugler I, Hu K, Bauer W, Eilles C, Ertl G. Time course of cardiac structural, functional and electrical changes in asymptomatic patients after myocardial infarction: their inter-relation and prognostic impact. J Am Coll Cardiol. 2001;38:33–40.
10. Muthupillai R, Flamm SD, Wilson JM, Pettigrew RI, Dixon WT. Acute myocardial infarction: tissue characterization with $T_{1\rho}$-weighted MR imaging - initial experience. Radiology. 2004;232:606–10.
11. van Oorschot JWM, El Aidi H, Jansen of Lorkeers SJ, Gho JM, Froeling M, Visser F, Chamuleau SA, Doevendans PA, Luijten PR, Lainer T, Zwanenburg JJ. Endogenous assessment of chronic myocardial infarction with $T_{1\rho}$-mapping in patients. J Cardiovasc Magn Reson. 2014;16:104–12.
12. Verhaert D, Thavendiranathan P, Giri S, Mihai G, Rajagopalan S, Simonetti OP, Raman SV. Direct T_2 quantification of myocardial edema in acute ischemic injury. JACC Cardiovasc Imaging. 2011;4:269–78.
13. de Roos A, van der Wall EE. Evaluation of ischemic heart disease by magnetic resonance imaging and spectroscopy. Radiol Clin N Am. 1994; 32:581–92.
14. Huber S, Muthupillai R, Lambert B, Pereyra M, Napoli A, Flamm SD. Tissue characterization of myocardial infarction using $T_{1\rho}$: influence of contrast dose and time of imaging after contrast administration. J Magn Reson Imaging. 2006;24:1040–6.
15. Abdel-Aty H, Zagrosek A, Schultz-Menger J, Taylor AJ, Messroghli D, Kumar A, Gross M, Dietz T, Friedrich MG. Delayed enhancement and T_2-weighted cardiovascular magnetic resonance imaging differentiate acute from chronic myocardial infarction. Circulation. 2004;109:2411–6.
16. Witschey WR, Zsido GA, Koomalsingh K, Kondo N, Minakawa M, Shuto T, McGarvey JR, Levack MM, Contijoch F, Pilla JJ, Gorman JH 3rd, Gorman RC. In vivo chronic myocardial infarction characterization by spin locked cardiovascular magnetic resonance. J Cardiovasc Magn Reson. 2012;14:37.
17. Witschey WR, Pilla JJ, Ferrari G, Koomalsingh K, Haris M, Himmon R, Zsido G, Gorman JH 3rd, Gorman RC, Reddy R. Rotating frame spin lattice relaxation in a swine model of chronic, left ventricular myocardial infarction. Magn Reson Med. 2010;64:1453–60.
18. Abdel-Aty H, Simonetti O, Friedrich MG. T_2-weighted cardiovascular magnetic resonance imaging. J Magn Reson Imaging. 2017;26:452–9.
19. Reimer KA, Jennings RB. The changing anatomic reference base of evolving myocardial infarction. Underestimation of myocardial collateral blood flow and overestimation of experimental anatomic infarct size due to tissue edema, hemorrhage and acute inflammation. Circulation. 1979;60:866–76.
20. Hakumäki JM, Gröhn OH, Tyynelä K, Valonen P, Ylä-Herttuala S, Kauppinen RA. Early gene therapy-induced apoptotic response in BT4C gliomas by magnetic resonance relaxation contrast T_1 in the rotating frame. Cancer Gene Ther. 2002;9:338–45.
21. Mustafa HSN, Dragneva G, Lottonen L, Merentie M, Petrov L, Heikura T, Ylä-Herttuala E, Ylä-Herttuala S, Gröhn O, Liimatainen T. Longitudinal rotating frame relaxation time measurements in infarcted mouse myocardium in vivo. Magn Reson Med. 2013;69:1389–95.
22. Liimatainen T, Sorce DJ, O'Donnell R, Michaeli S. MRI contrasts from relaxation along a fictitious field (RAFF). Magn Reson Med. 2010;64:983–94.
23. Liimatainen T, Hakkarainen H, Mangia S, Huttunen JM, Storino C, Idiyatullin D, Sorce D, Garwood M, Michaeli S. MRI contrasts in high rank rotating frames. Magn Reson Med. 2015;73:254–62.
24. Hakkarainen H, Sierra A, Mangia S, Garwood M, Michaeli S, Gröhn O, Liimatainen T. MRI relaxation in the presence of fictitious fields correlates with myelin content in normal rat brain. Magn Reson Med. 2016;75:161–8.
25. Gao E, Lei YH, Shang X, Huang ZM, Zuo L, Boucher M, Fan Q, Chuprun JK, Ma XL, Koch WJ. A novel and efficient model of coronary artery ligation and myocardial infarction in the mouse. Circ Res. 2010;107:1445–53.
26. Vaughan JT, Garwood M, Collins CM, Liu W, DelaBarre L, Adriany G, Andersen P, Merkle H, Goebel R, Smith MB, Urgurbil K. 7 T vs. 4 T: RF power, homogeneity, and signal-to-noise comparison in head images. Magn Reson Med. 2001;46:24–30.
27. Amano Y, Tachi M, Kumita S. Three-dimensional look-locker MRI for evaluation of postcontrast myocardial and blood T_1 values: comparison with two-dimensional look-locker and late gadolinium enhancement MRI. Acta Radiol. 2013;54:8–13.
28. Park C, Park EH, Chang K, Hong KS. Sector-based assessment of infarct size on late-gadolinium-enhancement MRI in a mouse model of acute myocardial infarction. Int Heart J. 2016;57:736–41.
29. Ugander M, Bagi PS, Oki AJ, Chen B, Hsu LY, Aletras AH, Shah S, Greiser A, Kellman P, Arai AE. Myocardial edema as detected by pre-contrast T1 andT2 CMR delineates area at risk associated with acute myocardial infarction. JACC Cardiovasc Imaging. 2012;5:595–603.
30. Liimatainen T, Sierra A, Hanson T, Sorce DJ, Ylä-Herttuala S, Garwood M, Michaeli S, Gröhn O. Glioma cell density in a rat gene therapy model gauged by water relaxation rate along a fictitious magnetic field. Magn Reson Med. 2012;67:269–77.
31. Kettunen MI, Sierra A, Närväinen MJ, Valonen PK, Ylä-Herttuala S, Kauppinen RA, Gröhn OH. Low spin-lock field T_1 relaxation in the rotating frame as a sensitive MR imaging marker for gene therapy treatment response in rat glioma. Radiology. 2007;243:796–803.
32. Bönner F, Jacoby C, Temme S, Borg N, Ding Z, Schrader J, Flögel U. Multifunctional MR monitoring of the healing process after myocardial infarction. Basic Res Cardiol. 2014;109:430.
33. Mäkelä HI, De Vita E, Gröhn OH, Kettunen MI, Kayec M, Lythgoe M, Garwood M, Ordidge R, Kauppinen RA. B0 dependence of the on-resonance longitudinal relaxation time in the rotating frame (T1rho) in protein phantoms and rat brain in vivo. Magn Reson Med. 2004;51:4–8.
34. Haberkorn SM, Jacoby C, Ding Z, Keul P, Bönner F, Polzin A, Levkau B, Schrader J, Kelm M, Flögel U. Cardiocascular magnetic resonance relaxometry predicts regional functional outcome after experimental myocardial infarction. Circ Cardiovasc Imaging. 2017;10:e006025.
35. Nahrendorf M, Hiller KH, Hu K, Ertl G, Haase A, Bauer WR. Cardiac magnetic resonance imaging in small animal models of human heart failure. Med Image Anal. 2003;7:369–75.